frontiers | Frontiers in Astronomy and Space Sciences

TYPE Original Research
PUBLISHED 26 July 2023
DOI 10.3389/fspas.2023.1232151

OPEN ACCESS

EDITED BY
Richard de Grijs,
Macquarie University, Australia

REVIEWED BY
Paolo Ventura,
Astronomical Observatory of Rome (INAF), Italy
Mario Gai,
Osservatorio Astrofisico di Torino (INAF), Italy

*CORRESPONDENCE
Bo Zhang,
zb@shao.ac.cn

RECEIVED 31 May 2023
ACCEPTED 03 July 2023
PUBLISHED 26 July 2023

CITATION
Sun Y, Zhang J, Zhang B, Xu S, Mai X, Ding H, Chen W and Wen S (2023), Miras as a distance indicator in the CSST, JWST, and Gaia era.
Front. Astron. Space Sci. 10:1232151.
doi: 10.3389/fspas.2023.1232151

Miras as a distance indicator in the CSST, JWST, and Gaia era

Yan Sun[1], Jingdong Zhang[1,2], Bo Zhang[1]*, Shuangjing Xu[3], Xiaofeng Mai[1,2], Hao Ding[1], Wen Chen[4,5] and Shiming Wen[1]

[1]Shanghai Astronomical Observatory, Chinese Academy of Sciences, Shanghai, China, [2]University of Chinese Academy of Sciences, Beijing, China, [3]Korea Astronomy and Space Science Institute, Daejeon, Republic of Korea, [4]Yunnan Observatories, Chinese Academy of Sciences, Kunming, Yunnan, China, [5]Yunnan Key Laboratory of the Solar physics and Space Science, Kunming, China

Mira variables are important distance indicators owing to the clear period–luminosity relation at infrared wavelengths. We have compiled a sample of 343 Galactic Miras selected from the American Association of Variable Star Observers database and Gaia Data Release 3. We used V-band observations from the American Association of Variable Star Observers to generate template light curves and derived mean magnitudes in the near-infrared JHK band from the Two Micron All-Sky Survey. Based on the Gaia-Two Micron All-Sky Survey diagram and the Gaia-LPV2 catalog, we classified 299 O-rich and 44 C-rich Miras. We fitted the Galactic period–luminosity relations for O-rich Miras in the near-infrared JHK band and estimated slopes (−2.74 ± 0.32, −3.14 ± 0.30, and −3.50 ± 0.25) and zero points (−5.58 ± 0.06 mag, −6.40 ± 0.06 mag, and −6.84 ± 0.05 mag) defined at logP (days) = 2.30, separately. Although the uncertainties of our derived Galactic PLRs for Miras are still larger than those of other galaxies, the multi-band sky survey conducted using the China Space Survey Telescope could help build more reliable and accurate PLRs for Miras, particularly in a near-infrared y band (927–1,080 nm).

KEYWORDS

AGB stars, Mira variable stars, Milky Way, period–luminosity relation, distance indicators

1 Introduction

Mira variables (Miras) are a class of late-type, long-period variables (LPVs). They are distributed in the coldest and brightest parts of the asymptotic giant branch (AGB). Miras typically have a pulsation period ranging from ~100 to 1,000 days and have a large amplitude variation $\Delta V > 2.5$ mag (Kholopov et al., 1985). The initial masses of Miras are typically lower than those of Cepheids (Feast, 2009), which suggests that Miras can be found in all types of galaxies. Furthermore, Miras are generally brighter than Cepheids in the infrared band (Feast and Whitelock, 2014), where period–luminosity relations (PLRs) are better constrained than those at the optical band owing to the reduced effect of dust at longer wavelengths (Glass and Evans, 1981). In the era of large space infrared telescopes, e.g., the James Webb Space Telescope (JWST), the JWST's higher sensitivity and resolution are great advantages to observing more Miras, particularly in supernova (SN) host galaxies. Miras observed with the JWST could be used to measure PLRs and extend the calibration distance of SNe Ia, improving our ability to measure the Hubble constant. Therefore, Miras will become an important tool for determining distances in the future.

Nevertheless, due to insufficient sampling or time range of some of the datasetsin the JWST, it is not enough to use only JWST data to obtain the accurate mean apparent

magnitude of Miras in the infrared band. According to the light-curve correction method, which could fit optical templates to the near-infrared (NIR) and mid-infrared data (Yuan et al., 2017, 2018; Iwanek et al., 2021a), we could fit a well-sampled optical template by using the optical V band data from the American Association of Variable Star Observers (AAVSO) to the sparsely sampled NIR data from the Two Micron Sky-Survey (2MASS) to calculate the true mean magnitude of Miras [see Sun et al. (2022) and Section 2.2 for more details]. The China Space Survey Telescope (CSST) will launch and begin its science operations around 2024, and the 10-year survey program of the CSST will cover approximately 17,500 square degrees of the sky in near ultraviolet (NUV), *u*, *g*, *r*, *i*, *z*, and *y* bands with a wavelength range of 255–1,000 nm (Zhan, 2021). Owing to its large field of view, the CSST has advantages in sky coverage and survey efficiency, so despite the difference in wavelength coverage compared to the 2MASS and JWST, using the CSST to study the PLRs for Miras is an option as well, and this allows for faster access to larger Mira samples. Furthermore, the photometric time series of Miras in the focal sky areas of the observation plan of the CSST can be obtained, benefits from which will be observed several times.

Miras have been widely studied as distance indicators in the Milky Way and extragalactic galaxies. Glass and Evans (1981) reported a PLR for Miras in the NIR band based on 11 Miras in the Large Magellanic Cloud (LMC). Feast et al. (1989) determined NIR PLRs for Miras based on 29 O-rich and 20 C-rich Miras in the LMC and found that the PLRs for O-Miras and C-Miras are very similar in the NIR *K* band. Based on massive compact halo object (MACHO) data, Wood et al. (1999) and Wood (2000) revealed five distinct, parallel sequences in the period–luminosity plane, and one of these sequences represented Miras [sequence C in Figure 1 of the work of Wood (2000)]. Later on, Whitelock et al. (2008) determined an NIR *K* band PLR for O-rich Miras in the LMC assuming a distance modulus of 18.39 ± 0.05 mag (van Leeuwen et al., 2007). Yuan et al. (2017) determined PLRs for O-rich Miras at near-infrared wavelengths assuming a distance modulus of 18.439 mag (Pietrzyński et al., 2013). A distance modulus of 18.477 ± 0.026 mag for the LMC was assumed by Pietrzyński et al. (2019), and Iwanek et al. (2021b) determined the mid-infrared PLRs in the range of 3.4–22 μm using 1194 C-rich and 469 O-rich Miras separately. Iwanek et al. (2021a) determined PLRs for Miras in 42 bands ranging from 0.1 to 40 μm using a sample of 29 O-rich and 111 C-rich Miras in the LMC. Assuming the PLR slope is the same as that of the LMC, zero points of the PLRs for Miras have also been determined in other galaxies, e.g., M 33 (Yuan et al., 2018), NGC 4258 (Huang et al., 2018), and NGC 1559 (Huang et al., 2020). Sun et al. (2022) determined the Galactic PLR for Miras in the NIR K band using 22 O-rich Miras with VLBI parallaxes.

However, there are still some issues regarding the use of PLR for Miras. First, according to recent studies (Ita and Matsunaga, 2011; Yuan et al., 2017, 2018), it seems that PLRs for Miras in different galaxies are insensitive to metallicity variations, and to validate this, an improved accuracy of PLR is mandatory. Second, due to the assumed LMC distance, e.g., the latest distance modulus of 18.477 ± 0.026 mag estimated by Pietrzyński et al. (2019), there might still be a systematic error in estimated distances for other galaxies using PLRs for LMC Miras. Therefore, if the PLR for Miras is universal, the zero point for the PLR should be better determined.

Having more than 90,000 LPVs with $\sigma_\pi/\pi < 0.15$ (Lebzelter et al., 2022), Gaia Data Release 3 (DR3) provides an opportunity to derive Galactic PLRs for Miras independent of other galaxies. In this paper, we collected NIR and optical data of 343 Miras in the Milky Way. Using their optical V-band observations, we generated template light curves and derived mean magnitudes in the NIR JHK band. Additionally, we classified our Miras sample into O-rich and C-rich Miras and derived NIR PLRs for O-rich Miras using Gaia DR3 parallaxes. The rest of the paper is organized as follows. In Section 2, we describe the data used in this paper and introduce the procedure to generate mean apparent magnitude in the NIR band. In Section 3, we classify our Mira sample into O- and C-rich Miras and present PLRs in the NIR band for O-rich Miras. In Section 4, we compare our Galactic Miras PLRs with those in other galaxies and discuss how to use the CSST sky survey to improve the accuracy of Galactic Miras PLRs in the future. A summary and outlook on studying PLRs for Miras using the CSST are presented in Section 5.

2 Data

2.1 Sample selection and period determination

We have collected our Miras sample from the AAVSO,[1] which could provide long-period photometry data in the optical *V* band. The NIR data are taken from the 2MASS (Skrutskie et al., 2006) which observed the celestial sphere in three NIR *JHK* bands. Gaia DR3 provides astrometric parameters for approximately 1,468 million sources with a median parallax uncertainty of approximately 0.02–0.03 mas at magnitude $G = 9$–14 (Gaia Collaboration et al., 2021). By combining the optical data of AAVSO, the parallax of Gaia DR3, and the NIR data of 2MASS, we could obtain a large number of Galactic Miras with distance and apparent magnitude in optical and NIR bands.

For optical data, we selected those sources with more than 1,000 measurements in the optical V band to better determine the period for Miras. For the parallax, we focused on sources with positive parallax and $\sigma_\pi/\pi \leq 10\%$, where π and σ_π are the parallax and its uncertainty, respectively. We also adopted the systematic zero-point correction of Gaia parallaxes (π_0) (Lindegren et al., 2021) for each source in our sample. For NIR data, we only selected those sources with *J*, *H*, and *K* band magnitudes. Finally, we selected 343 Miras for our sample, and the sky distribution of the Miras sample is presented in Figure 1.

For the determination of the periods of Miras in our sample, optical data in the *V* band provided by the AAVSO were used. There are multiple methods to derive the period of non-uniform interval sampled time series, for example, the Lomb–Scargle periodogram (Lomb, 1976; Scargle, 1982). Herein, an alternative method is adopted to verify the periods provided by the AAVSO, and since the Miras we selected have all been observed continuously for a long time, using different methods does not change the result much. We averaged and interpolated the time series and then conducted fast Fourier transform (FFT) to derive the periods. The

1 https://www.aavso.org

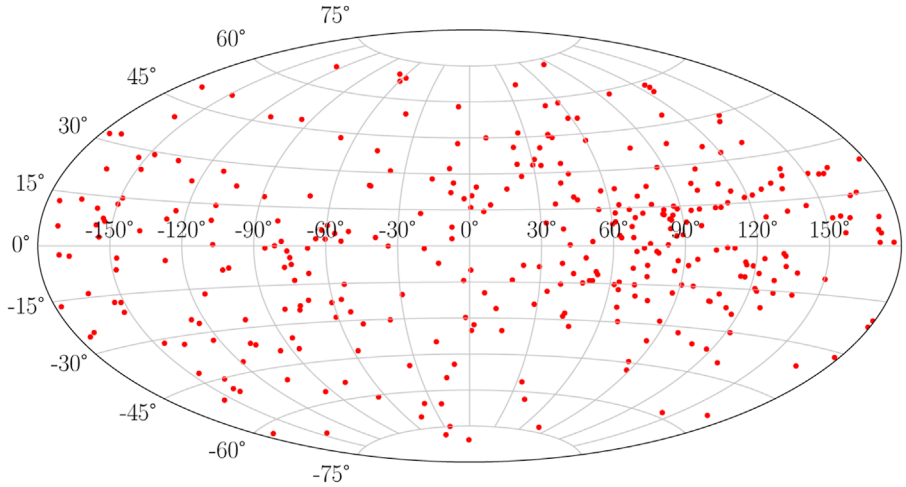

FIGURE 1
Sky distribution of our Miras sample (red points) in Galactic coordinates.

raw time series are first averaged with an interval of 30 days and then interpolated with the smoothing spline fit function provided by SciPy (Virtanen et al., 2020). Outliers are inevitable in the result of spline interpolation of data series with noises; hence, we replaced the outliers with medians, with identification criteria as follows:

$$|\Delta M_V| > T \tag{1}$$

and

$$T = \begin{cases} 3, & \sigma_{M_V} > 3 \\ \sigma_{M_V}, & 1.5 \le \sigma_{M_V} \le 3 \\ 1.5, & \sigma_{M_V} < 1.5, \end{cases} \tag{2}$$

where ΔM_V is the difference between the data points and the medians of interpolated V-band series, while σ_{M_V} is the standard deviation of the series. After the aforementioned pre-processing procedure, the periods of our sample can then be calculated through FFT. Figure 2 shows the period difference between the result and the value provided by the AAVSO, in which the mean and standard deviation are 0.6 and 6.4 days, respectively, excluding four Miras (AC Aur, RW Pup, SW Peg, and WY Cas) due to their low magnitude data quality. The periods of these four Miras are replaced with the value obtained from the General Catalog of Variable Stars [GCVS; Samus et al. (2017)] database in the following analysis. Although there is no significant difference between the periods provided by our method and AAVSO for most of the sources in our Miras sample, the phase-folded light curves based on the periods provided by our method show a lower dispersion for a number of Miras. Figure 3 shows the phase-folded light curves based on the periods provided by our method and the AAVSO for Miras BH Cru. Therefore, we adopted the periods given by our method for the following analyses.

Figure 4 shows examples of 12 phase-folded light curves using pulsation periods determined by the aforementioned method in the *V* band of Miras in our sample.

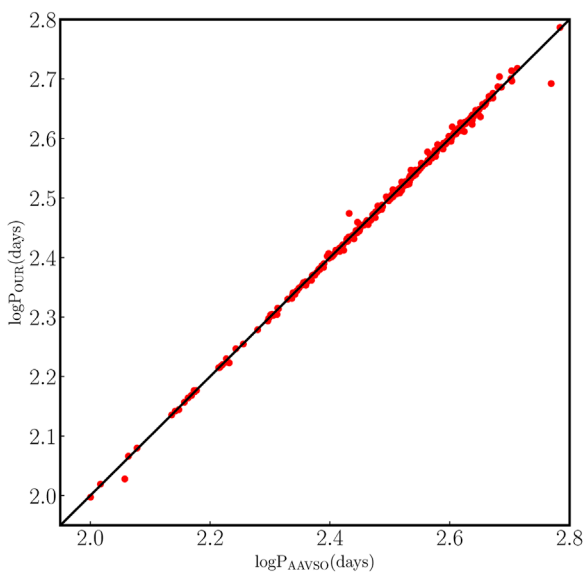

FIGURE 2
Comparison between the periods given by our method and the AAVSO separately. Each red point represents a Mira, and the diagonal line denotes $\log P_{OUR} = \log P_{AAVSO}$ on the scatter plot.

2.2 Mean magnitude in the NIR

Since Miras vary by an upward magnitude of 1 mag at 2 μm and 2MASS measurements are only at one epoch, this leads to extra uncertainty in the mean magnitude owing to periodic variations. In order to estimate a mean apparent magnitude in the NIR band, we adopted a method similar to that demonstrated by Yuan et al. (2017, 2018) and Iwanek et al. (2021a). This light curve correction method assumed that the shape of light curves in the NIR band for a Mira is the same as in the optical band, and variability is simply scaled,

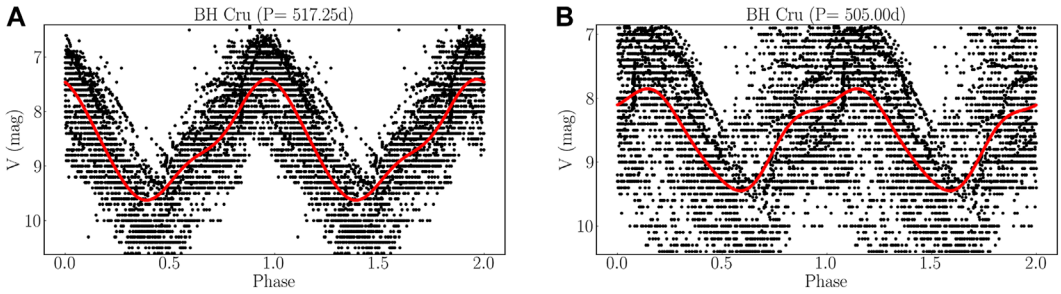

FIGURE 3
Example of the phase-folded light curve based on the periods provided by our method **(A)** and the AAVSO **(B)** in the V band for Miras BH Cru. Red solid line shows the modeled optical light curve.

shifted in magnitude, and shifted in phase of the optical band light curve. As shown in Figure 5, using long-period optical data in the *V* band provided by the AAVSO, we estimated the modeled optical light curve for a Mira. Then, we converted the modeled optical light curve to a near-infrared one using an amplitude ratio and a phase-lag between optical and NIR bands determined by Iwanek et al. (2021a); then, an infrared phase-adjusted constant was added to the measured magnitude; finally, the mean magnitude for a Mira could be obtained. Figure 5 shows an example of the light curve correction to mean magnitude for Mira R.

Interstellar extinction has a strong influence on stellar light and should be taken into account when determining the mean magnitude in the NIR band. Herein, we adopted the extinction parameters provided using the MW dust[2] (Bovy et al., 2016) algorithm. This algorithm can determine the extinction value at a given Galactic longitude, latitude, and distance by using three-dimensional dust maps (Drimmel et al., 2003; Marshall et al., 2006; Green et al., 2015). Together with the mean wavelength of the 2MASS *J*, *H*, and *K* (Skrutskie et al., 2006) and Gaia parallax, we could derive the extinction parameter A_{JHK} for our Miras sample. Combining with the mean magnitude and extinction parameter in the NIR band, we obtained the absolute magnitude M_{JHK} in the NIR band for a matched Mira and estimated the uncertainty by taking into account the uncertainties from both 2MASS measurements and the amplitude ratio and phase lag for light curve correction.

3 Results

3.1 Classification of O-rich and C-rich Miras

Miras are usually divided into O-rich and C-rich stars. The most common method to distinguish the O-rich and C-rich Miras in the LMC is using NIR photometry (J–K) from the 2MASS (Skrutskie et al., 2006). However, due to the large depth of the Galactic disk and bulge along the line of sight (Soszyński et al., 2013), the same method could not be used for Miras in the Milky Way. In order to classify O-rich and C-rich Miras in our sample, we adopted a so-called Gaia–2MASS diagram (Lebzelter et al., 2018; Abia et al., 2020, 2022) which combines Gaia and 2MASS photometry. This diagram was originally designed by Lebzelter et al. (2018) and is suitable to distinguish different kinds of AGB stars according to mass and chemistry (i.e., O- and C-rich). In the Gaia–2MASS diagram, the absolute magnitude M_K is correlated with a combination of Gaia and 2MASS photometry $W_{RP,BP-RP} - W_{K,J-K}$, which are defined as

$$W_{RP,BP-RP} = G_{RP} - 1.3\,(G_{BP} - G_{RP}) \tag{3}$$

and

$$W_{K,J-K} = K - 0.686\,(J - K)\,, \tag{4}$$

where $W_{RP,BP-RP}$ and $W_{K,J-K}$ are reddening free Wesenheit functions (Soszyński et al., 2005; Lebzelter et al., 2018) and G_{BP} and G_{RP} are the magnitudes of Gaia BP and RP bands, respectively. The passband of the BP filter is centered at shorter wavelengths than the passband of the RP filter (Riello et al., 2021), so BP–RP indicates the color of a star. The distribution in the Gaia–2MASS diagram of our sample is shown in Figure 6, where we found that O- and C-rich Miras are distributed in different regions, which could be easily distinguished. The clear separation between O-rich and C-rich Miras in Figure 6 relates to distinct molecular absorption features in their spectra and different evolutionary properties (Lebzelter et al., 2018). In addition, Lebzelter et al. (2022) provided the second Gaia catalog of LPVs (hereafter, Gaia-LPV2) which contains 720,558 LPV candidates, including 546,468 stars classified as C-star candidates. As shown in Figure 6, we cross-matched the Gaia-LPV2 catalog with our sample and found that the classification of C-rich Miras based on both Gaia-LPV2 and Gaia–2MASS diagrams is in good agreement. Only five O-rich Miras classified by the Gaia–2MASS diagram are discrepantly classified as C-rich Miras in Gaia-LPV2. We classified these five Miras as C-rich star. Finally, we selected 343 Miras for the following research. In our Miras sample, the re-determined periods of Miras ranged from 100 to 600 days, the *G* band magnitudes of Gaia DR3 ranged from 4 to 11 mag, and the distances are mostly within 3 kpc. Using the Gaia–2MASS diagram and the second Gaia catalog of LPVs, we found 299 O-rich and 44 C-rich Miras in our sample.

2 https://github.com/jobovy/mwdust

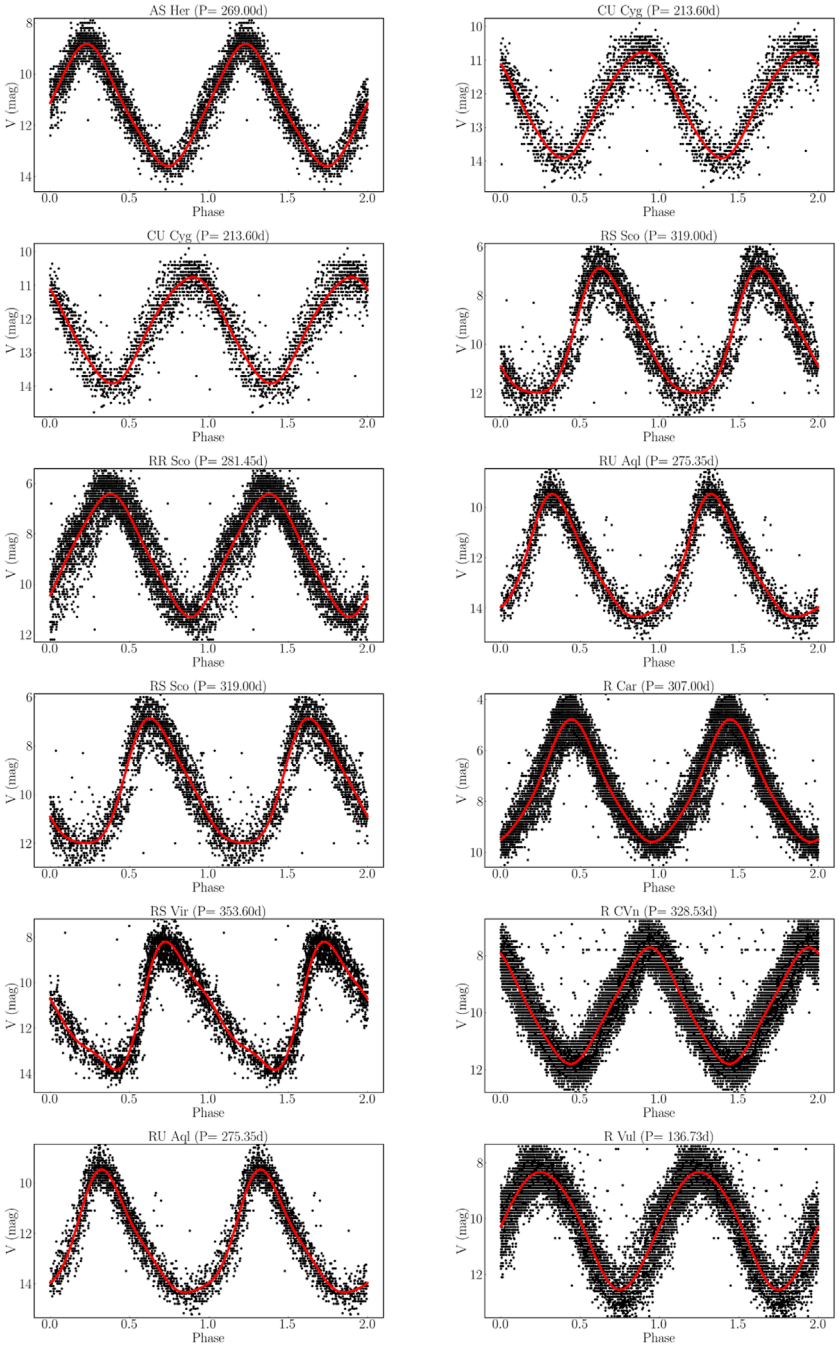

FIGURE 4
Phase-folded light curves with pulsation periods P (provided above each panel) in the *V* band for 12 examples of Miras from our sample. Red solid line shows the modeled optical light curve.

3.2 Miras PLRs in the NIR band

Considering that we only have 44 C-rich Miras and most of their periods are concentrated in 400 ~500 days, we focused on O-rich Miras in this paper and fit the O-rich Mira PLRs based on 299 O-rich Miras. The recent analysis conducted by Iwanek et al. (2021a,b) found the O-rich Miras whose P < 400 days can be well described by a linear PLR. Approximately 90{%} of the O-rich Miras pulsation period in our sample is less than 400 days. Furthermore, in order to compare our O-rich PLRs with existing PLRs in the literature, the PLR formula is defined as

$$M_{JHK} = a_0 + a_1\,(logP - 2.3) \tag{5}$$

to match those of the work of Yuan et al. (2017), Lebzelter et al. (2018), and Iwanek et al. (2021a), where M_{JHK} is the absolute

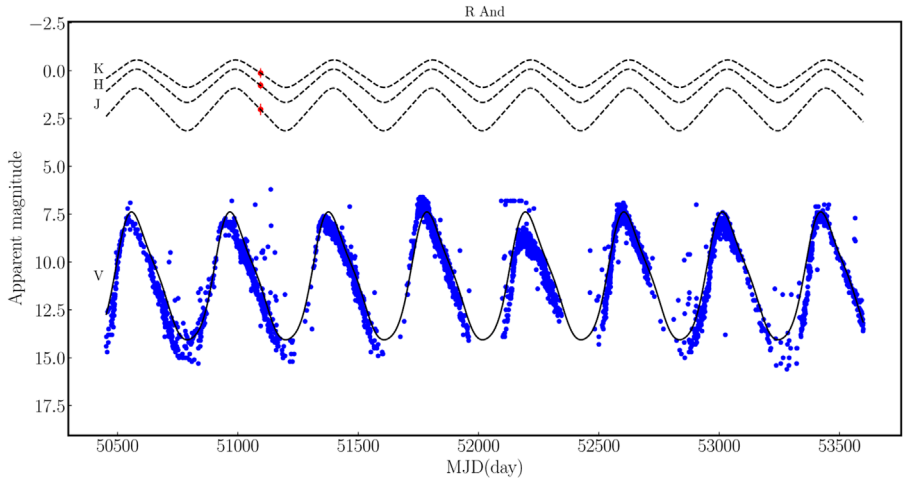

FIGURE 5
Example of the light curve at the optical V band (*lower solid line for model and dots for data*) and the model near-infrared *JHK* band (*upper dashed lines*) for Miras R. Single-epoch 2MASS data are shown in red. Solid line shows the modeled optical light curve. Dashed line shows the near-infrared light curve converted from the modeled optical light curve.

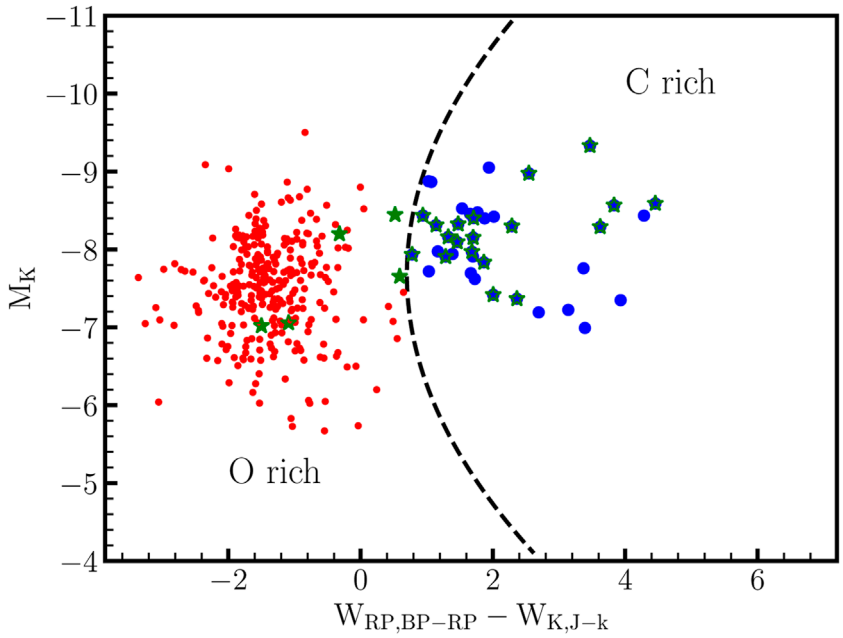

FIGURE 6
Gaia−2MASS diagram for our sample. Curved dashed line represents the theoretical limit between O-rich (left of the line) and C-rich Miras (right of the dashed line). Red points represent the O-rich Miras, and the blue points represent the C-rich Miras classified by Gaia−2MASS in our sample. Green stars represent the C-rich Miras in the Gaia-LPV2 catalog.

magnitude in the NIR *JHK* band, P is the period, and a_0 and a_1 are the zero-point slope of the PLR.

For PLR fitting, we used a Bayesian MCMC approach which is similar to the approach used by Sun et al. (2022) with prior information: slope −3.60 ± 1.00 and zero point −6.90 ± 1.00 mag at logP (days) = 2.30. Table 1 lists the parameters from the determined Galactic PLR and recently published PLRs for O-rich Miras in the NIR band for different galaxies. The results for the LMC by Yuan et al. (2017) were based on Miras with periods <400 days, assuming the distance modulus of 18.493 ± 0.048 mag (Pietrzyński et al., 2013). We have adjusted the zero point and its uncertainty to an updated distance modulus of

TABLE 1 NIR PLRs for O-rich Miras.

Galaxies	Band	a_1	a_0	Scatter	Number	Reference
Milky Way	*J*	−2.74 ± 0.32	−5.58 ± 0.06	0.51	299	This paper
	H	−3.14 ± 0.30	−6.40 ± 0.06	0.45	299	This paper
	K	−3.50 ± 0.25	−6.84 ± 0.05	0.42	298	This paper
LMC	*J*	−3.48 ± 0.09	−5.80 ± 0.04	0.15	158	Yuan et al. (2017)
M 33	*J*	[−3.48]	−5.90 ± 0.01	0.25	1,169	Yuan et al. (2018)
LMC	*H*	−3.64 ± 0.09	−6.57 ± 0.04	0.16	158	Yuan et al. (2017)
M 33	*H*	[−3.64]	−6.65 ± 0.01	0.24	1,169	Yuan et al. (2018)
LMC	*K*	−3.77 ± 0.07	−6.92 ± 0.04	0.12	158	Yuan et al. (2017)
M 33	*K*	[−3.77]	−6.97 ± 0.01	0.21	1,169	Yuan et al. (2018)
LMC	*J*	−1.83 ± 0.79	−5.52 ± 0.09	0.46	29	Iwanek et al. (2021a)
LMC	*K*	−3.30 ± 0.46	−6.67 ± 0.06	0.27	29	Iwanek et al. (2021a)

Columns 1 and 2 list the galaxies and NIR band for Miras' PLR. Columns 3 and 4 provide the PLR slopes and zero points. Columns 5 and 6 list the standard deviation of the post-fit residuals in magnitudes and the number of Miras fitted. The results for the LMC in the work of Yuan et al. (2017) were based on Miras with periods < 400 days, assuming a distance modulus of 18.493 ± 0.048 mag (Pietrzyński et al., 2013); we have adjusted the zero point and its uncertainty to an updated distance modulus of 18.477 ± 0.026 mag (Pietrzyński et al., 2019). The slope of PLR for M 33 in the work of Yuan et al. (2018) was fixed to match the LMC slope determined by Yuan et al. (2017). The PLR for the LMC conducted by Iwanek et al. (2021a) assumed a distance modulus of 18.477 ± 0.026 mag (Pietrzyński et al., 2019); the zero-point uncertainty includes both statistical and systematic errors.

18.477 ± 0.026 mag (Pietrzyński et al., 2019). The slope of the PLR for M 33 by Yuan et al. (2018) was fixed to match the LMC slope determined by Yuan et al. (2017). The PLR for the LMC in the work of Iwanek et al. (2021a) assumed a distance modulus of 18.477 ± 0.026 mag (Pietrzyński et al., 2019); the zero-point uncertainty includes both statistical and systematic errors. The absolute magnitudes for each O-rich Miras and the best-fit PLRs in the NIR band are presented in Figure 7. As shown in Table 1, it is clear that as the wavelength increases, the value of the PLR slope and the scatter of PLR post-fit residuals decrease. This is consistent with the previous research result demonstrated by Iwanek et al. (2021a).

4 Discussion

As shown in Table 1, although the slopes of PLRs are slightly different in different galaxies, the zero points of PLRs for the Milky Way are statistically consistent with those for the LMC or M 33. The scatter of PLR post-fit residuals for Galactic Miras is larger than that for the LMC or M 33. One likely reason is that the Miras in other galaxies used the same distance modulus, which removes distance uncertainty as a source of scatter. By contrast, our Galactic Miras used individual parallax from Gaia DR3. Another reason is that our Miras sample has only a single epoch of the 2MASS photometric measurement, and we used light-curve correction method, as described in Section 2.2, to obtain a more reliable apparent magnitude in the NIR band. Since the AAVSO's optical band data come from different observers around the world, these optical band photometric measurements used in the light-curve correction method could bring some systematic errors in the estimated mean magnitude in the NIR band. This could lead to a larger scatter in the residuals of PLR fitting. Furthermore, our Miras sample throughout the Milky Way is affected by a significant spread in extinction, which also has an impact on the scatter of PLR post-fit residuals.

In the future, the multi-band imaging survey of the CSST will cover a wavelength range of 0.255–1.0 μm, which is divided into seven bands (Zhan, 2021). According to the operation simulation of the progress of the imaging survey of the CSST, approximately 12,000 square degrees of the sky will be covered by any band filter at least once in the first year, and over 17,500 square degrees of the sky will completely be covered by all band filters at a given number of times during the 10-year mission. This provides an opportunity to compile a catalog containing a large number of Miras and their apparent magnitudes in CSST wavebands. We will be able to construct a more accurate light-curve correction method for studying the amplitude ratio and phase lag as a function of wavelength for Miras in CSST wavebands. Furthermore, the accuracy of the NIR magnitude of the Miras will be improved by using the amplitude ratio and phase lag of Miras in CSST wavebands. In particular, directly measured magnitude time series at the wavelength of approximately 1 μm (CSST *y*-band, 927–1,080 nm) will yield more precise mean magnitudes and establish an independent PLR for Miras in a unique waveband and typical magnitude range. The CSST spectral survey will also be helpful in establishing a more accurate local extinction correction, which will improve the measurement accuracy of all related parameters. The CSST will also provide an opportunity to compare PLRs for different galaxies. Since the main target of the first-stage survey is other galaxies, a sample of Miras in different galaxies can be collected. This Mira sample has a high internal consistency and is suitable for the comparison between galaxies. Therefore, we can study whether PLRs for different galaxies are significantly inconsistent and are the causes for the discrepancy.

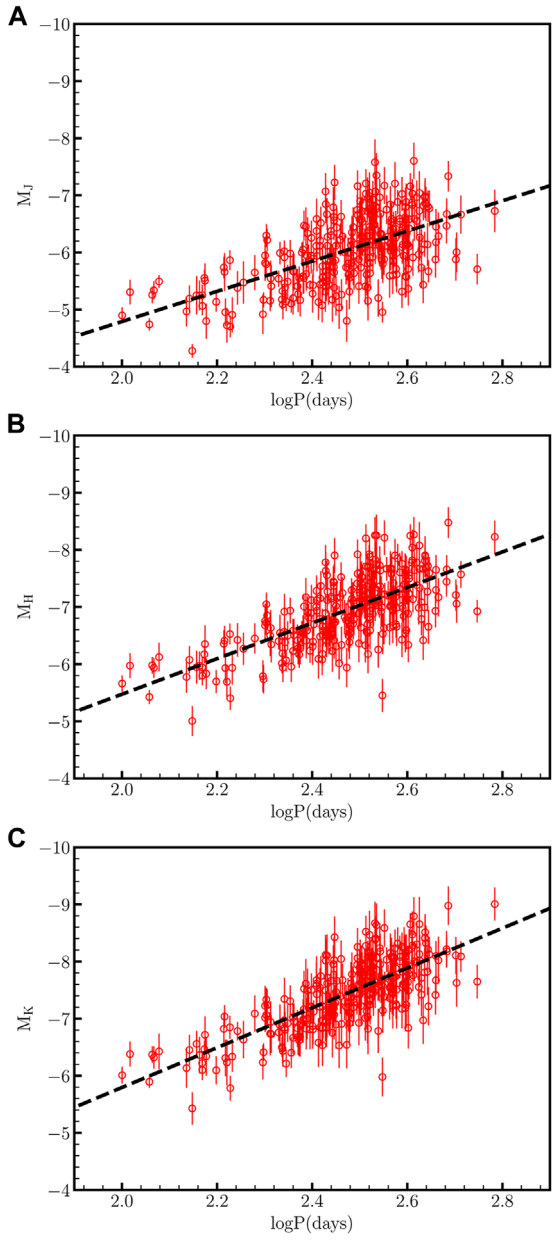

FIGURE 7
PLRs for Galactic O-rich Miras at *J* **(A)**, *H* **(B)**, and *K* **(C)** bands using Gaia DR3 parallaxes. Dashed lines denote the fitted PLRs listed in Table 1.

5 Summary and outlook

In this paper, we studied the NIR PLRs using 343 Miras in the Milky Way. For each star, we modeled the AAVSO *V*-band data to estimate the period of Miras. Then, using the modeled optical light curve, amplitude ratio, and a phase lag between optical and NIR bands, we obtain the mean magnitude of Miras in the NIR band. In order to classify the O-rich and C-rich Miras, we adopted a so-called Gaia-2MASS diagram and found 299 O-rich Miras and 44 C-rich Miras. Using 299 O-rich Miras, we derived PLRs for Miras in the NIR band and found that the slope of PLRs and the scatter of PLR post-fit residuals decrease with the increase in wavelength.

Miras vary by approximately 1 mag even in the NIR *K*-band. Although we used the light curve correction to obtain the mean magnitude in the NIR band for Miras, the uncertainty of absolute magnitudes is approximately ±0.3 mag when using only a single epoch from 2MASS. This usually dominates over parallax uncertainty when estimating absolute magnitudes.

The CSST survey program will offer a significant value in the study of Miras PLRs. The independent photometry conducted in various wavebands by the CSST presents a unique opportunity to investigate the multi-wavelength properties of Miras with a highly consistent dataset. It is noteworthy that the CSST survey will conduct key observations for some nearby galaxies, thereby making multi-epoch photometry available for Miras in these galaxies across all wavelength bands. By deriving the mean magnitudes and PLRs in all CSST-covered bands, we could obtain a comprehensive understanding of Miras' characteristics. Although the early stages of the CSST survey do not focus on the Milky Way, there is hope that a low-Galactic-latitude survey will be conducted in the future. This will provide a new batch of Mira samples in the Milky Way for further extensions of Miras PLRs. Miras with improved mean magnitudes from the CSST should increase the NIR band Mira PLR slope and zero-point accuracy by approximately 2~ 4 times. Meanwhile, the study of Miras distributed in different galaxies may address the question of whether Miras PLRs vary across galaxies. Although the CSST's current limited wavelength coverage in the NIR band means that the direct study of Miras PLRs at $\lambda > 1\ \mu$m is not feasible yet, the light-curve correction method could be used for the moment. Fortunately, the ability of the CSST to dock with China's space station provides an opportunity to upgrade its scientific instruments. Installing new instruments that cover a wider wavelength range in the NIR band would greatly enhance the CSST's potential to study PLRs for Miras.

Data availability statement

The original contributions presented in the study are included in the article/Supplementary Material; further inquiries can be directed to the corresponding author.

Author contributions

BZ proposed and improved the overall idea and framework of this work. YS and JZ were responsible for data acquisition, analysis, and final fitting results for the work. Other authors evaluated the results of this work. All authors contributed to the article and approved the submitted version.

Funding

This work was supported by the National Natural Science Foundation of China (NSFC) under grant no. U2031212 and 11903079. Funding for the DPAC was provided by national institutions, in particular the institutions participating in the *Gaia* Multilateral Agreement.

Acknowledgments

The authors acknowledge the variable star observations from the AAVSO International Database contributed by observers worldwide and used in this research. This work made use of data from the European Space Agency (ESA) mission *Gaia* (https://www.cosmos.esa.int/gaia) and processed by the *Gaia* Data Processing and Analysis Consortium (DPAC, https://www.cosmos.esa.int/web/gaia/dpac/consortium).

Conflict of interest

The authors declare that the research was conducted in the absence of any commercial or financial relationships that could be construed as a potential conflict of interest.

Publisher's note

Supplementary material

The Supplementary Material for this article can be found online at: https://www.frontiersin.org/articles/10.3389/fspas.2023.1232151/full#supplementary-material

References

Abia, C., de Laverny, P., Cristallo, S., Kordopatis, G., and Straniero, O. (2020). Properties of carbon stars in the solar neighbourhood based on Gaia DR2 astrometry. *aap* 633, A135. doi:10.1051/0004-6361/201936831

Abia, C., de Laverny, P., Romero-Gómez, M., and Figueras, F. (2022). Characterisation of Galactic carbon stars and related stars from Gaia EDR3. *aap* 664, A45. doi:10.1051/0004-6361/202243595

Bovy, J., Rix, H.-W., Green, G. M., Schlafly, E. F., and Finkbeiner, D. P. (2016). On galactic density modeling in the presence of dust extinction. *apj* 818, 130. doi:10.3847/0004-637X/818/2/130

Drimmel, R., Cabrera-Lavers, A., and López-Corredoira, M. (2003). A three-dimensional Galactic extinction model. *aap* 409, 205–215. doi:10.1051/0004-6361:20031070

Gaia Collaboration, Brown, A. G. A., Vallenari, A., Prusti, T., de Bruijne, J. H. J., Babusiaux, C., et al. (2021). Gaia early data Release 3. Summary of the contents and survey properties. *aap* 649, A1. doi:10.1051/0004-6361/202039657

Feast, M. W., Glass, I. S., Whitelock, P. A., and Catchpole, R. M. (1989). A period-luminosity-colour relation for Mira variables. *mnras* 241, 375–392. doi:10.1093/mnras/241.3.375

Feast, M., and Whitelock, P. A. (2014). "Variable stars and galactic structure," in *Setting the scene for Gaia and LAMOST*. Editors S. Feltzing, G. Zhao, N. A. Walton, and P. Whitelock., 298, 40–52. doi:10.1017/S17439213130-06182

Feast, M. W. (2009). "The ages, masses, evolution and kinematics of Mira variables," in *AGB stars and related phenomena*. Editors T. Ueta, N. Matsunaga, and Y. Ita, 48.

Glass, I. S., and Evans, T. L. (1981). A period-luminosity relation for Mira variables in the large magellanic Cloud. *nat* 291, 303–304. doi:10.1038/291303a0

Green, G. M., Schlafly, E. F., Finkbeiner, D. P., Rix, H.-W., Martin, N., Burgett, W., et al. (2015). A three-dimensional map of Milky Way dust. *apj* 810, 25. doi:10.1088/0004-637X/810/1/25

Huang, C. D., Riess, A. G., Hoffmann, S. L., Klein, C., Bloom, J., Yuan, W., et al. (2018). A near-infrared Period-Luminosity relation for Miras in NGC 4258, an anchor for a new distance ladder. *apj* 857, 67. doi:10.3847/1538-4357/aab6b3

Huang, C. D., Riess, A. G., Yuan, W., Macri, L. M., Zakamska, N. L., Casertano, S., et al. (2020). Hubble space telescope observations of Mira variables in the SN Ia host NGC 1559: An alternative candle to measure the Hubble constant. *apj* 889, 5. doi:10.3847/1538-4357/ab5dbd

Ita, Y., and Matsunaga, N. (2011). Period-magnitude relation of Mira-like variables in the Large Magellanic Cloud as a tool to understanding circumstellar extinction. *mnras* 412, 2345–2352. doi:10.1111/j.1365-2966.2010.18056.x

Iwanek, P., Kozłowski, S., Gromadzki, M., Soszyński, I., Wrona, M., Skowron, J., et al. (2021a). Multiwavelength properties of Miras. *apjs* 257, 23. doi:10.3847/1538-4365/ac1797

Iwanek, P., Soszyński, I., and Kozłowski, S. (2021b). Mid-infrared Period-Luminosity Relations for Miras in the large magellanic Cloud. *apj* 919, 99. doi:10.3847/1538-4357/ac10c5

Kholopov, P. N., Samus, N. N., Kazarovets, E. V., and Perova, N. B. (1985). The 67th name-list of variable stars. *Inf. Bull. Var. Stars* 2681, 1.

Lebzelter, T., Mowlavi, N., Lecoeur-Taibi, I., Trabucchi, M., Audard, M., García-Lario, P., et al. (2022). *Gaia data Release 3: The second Gaia catalogue of long-period variable candidates*. arXiv e-prints , arXiv:2206.05745.

Lebzelter, T., Mowlavi, N., Marigo, P., Pastorelli, G., Trabucchi, M., Wood, P. R., et al. (2018). A new method to identify subclasses among AGB stars using Gaia and 2MASS photometry. *aap* 616, L13. doi:10.1051/0004-6361/201833615

Lindegren, L., Bastian, U., Biermann, M., Bombrun, A., de Torres, A., Gerlach, E., et al. (2021). Gaia Early Data Release 3. Parallax bias versus magnitude, colour, and position. *aap* 649, A4. doi:10.1051/0004-6361/202039653

Lomb, N. R. (1976). Least-squares frequency analysis of unequally spaced data. *apss* 39, 447–462. doi:10.1007/BF00648343

Marshall, D. J., Robin, A. C., Reylé, C., Schultheis, M., and Picaud, S. (2006). Modelling the Galactic interstellar extinction distribution in three dimensions. *aap* 453, 635–651. doi:10.1051/0004-6361:20053842

Pietrzyński, G., Graczyk, D., Gallenne, A., Gieren, W., Thompson, I. B., Pilecki, B., et al. (2019). A distance to the Large Magellanic Cloud that is precise to one per cent. *nat* 567, 200–203. doi:10.1038/s41586-019-0999-4

Pietrzyński, G., Graczyk, D., Gieren, W., Thompson, I. B., Pilecki, B., Udalski, A., et al. (2013). An eclipsing-binary distance to the Large Magellanic Cloud accurate to two per cent. *nat* 495, 76–79. doi:10.1038/nature11878

Riello, M., De Angeli, F., Evans, D. W., Montegriffo, P., Carrasco, J. M., Busso, G., et al. (2021). Gaia early data Release 3. Photometric content and validation. *aap* 649, A3. doi:10.1051/0004-6361/202039587

Samus, N. N., Kazarovets, E. V., Durlevich, O. V., Kireeva, N. N., and Pastukhova, E. N. (2017). General catalogue of variable stars: Version GCVS 5.1. *Astron. Rep.* 61, 80–88. doi:10.1134/S1063772917010085

Scargle, J. D. (1982). Studies in astronomical time series analysis. II. Statistical aspects of spectral analysis of unevenly spaced data. *apj* 263, 835–853. doi:10.1086/160554

Skrutskie, M. F., Cutri, R. M., Stiening, R., Weinberg, M. D., Schneider, S., Carpenter, J. M., et al. (2006). The two Micron all sky survey (2MASS). *aj* 131, 1163–1183. doi:10.1086/498708

Soszyński, I., Udalski, A., Kubiak, M., Szymański, M. K., Pietrzyński, G., Żebruń, K., et al. (2005). The optical gravitational lensing experiment. Miras and semiregular variables in the large magellanic Cloud. *actaa* 55, 331–348. doi:10.48550/arXiv.astro-ph/0512578

Soszyński, I., Udalski, A., Szymański, M. K., Kubiak, M., Pietrzyński, G., Wyrzykowski, Ł., et al. (2013). The optical gravitational lensing experiment. The OGLE-III catalog of variable stars. XV. Long-period variables in the galactic bulge. *actaa* 63, 21–36. doi:10.48550/arXiv.1304.2787

Sun, Y., Zhang, B., Reid, M. J., Xu, S., Wen, S., Zhang, J., et al. (2022). A very long baseline array trigonometric parallax for RR aql and the Mira Period-Luminosity relation. *apj* 931, 74. doi:10.3847/1538-4357/ac69e0

van Leeuwen, F., Feast, M. W., Whitelock, P. A., and Laney, C. D. (2007). Cepheid parallaxes and the Hubble constant. *mnras* 379, 723–737. doi:10.1111/j.1365-2966.2007.11972.x

Virtanen, P., Gommers, R., Oliphant, T. E., Haberland, M., Reddy, T., Cournapeau, D., et al. (2020). SciPy 1.0: Fundamental algorithms for scientific computing in Python. *Nat. Methods* 17, 261–272. doi:10.1038/s41592-019-0686-2

Whitelock, P. A., Feast, M. W., and Van Leeuwen, F. (2008). AGB variables and the Mira period-luminosity relation. *mnras* 386, 313–323. doi:10.1111/j.1365-2966.2008.13032.x

Wood, P. R., Alcock, C., Allsman, R. A., Alves, D., Axelrod, T. S., Becker, A. C., et al. (1999). "MACHO observations of LMC red giants: Mira and semi-regular pulsators, and contact and semi-detached binaries," in *Asymptotic giant branch stars*. Editors T. Le Bertre, A. Lebre, and C. Waelkens, 191,151.

Wood, P. R. (2000). Variable red giants in the LMC: Pulsating stars and binaries? *pasa* 17, 18–21. doi:10.1071/AS00018

Yuan, W., Macri, L. M., He, S., Huang, J. Z., Kanbur, S. M., and Ngeow, C.-C. (2017). Large magellanic Cloud near-infrared synoptic survey. V. Period-luminosity Relations of Miras. *aj* 154, 149. doi:10.3847/1538-3881/aa86f1

Yuan, W., Macri, L. M., Javadi, A., Lin, Z., and Huang, J. Z. (2018). Near-infrared Mira Period-Luminosity Relations in M33. *aj* 156, 112. doi:10.3847/1538-3881/aad330

Zhan, H. (2021). The wide-field multiband imaging and slitless spectroscopy survey to be carried out by the survey space telescope of China manned space program. *Chin. Sci. Bull.* 66, 1290–1298. doi:10.1360/TB-2021-0016